PPARG PROTEIN EXPRESSION IN ADVANCED UROTHELIAL CARCINOMA MAY PROVIDE A PRECISION APPROACH TO POTENTIALLY SELECT FOR RESPONSE TO FX-909, A FIRST-IN-CLASS PPARG-TARGETING AGENT

Abstract #856

Evisa Gjini*, William Motley*‡, Adarsh Joshi, Bijal Kakrecha, Jennifer Mertz, Kaylyn Williamson, Stefan Kirov, Michaela Bowden

Flare Therapeutics, Cambridge, Massachusetts

*Co-primary authors; ‡Employee of Flare Therapeutics at the time this study was performed

BACKGROUND

- FX-909, a PPARG inverse agonist, has demonstrated robust preclinical activity in xenograft models and is currently being evaluated in a first-in-human, dose-escalation and expansion study in patients with advanced urothelial carcinoma (UC; NCT05929235)[1].
- PPARG drives development of Urothelial Carcinoma with luminal differentiation.
- In Muscle-Invasive Urothelial Carcinoma (MIUC), PPARG expression is associated with the luminal lineage, which accounts for ~65% of all advanced UC patients[2].
- An immunohistochemistry (IHC) prototype assay was developed to detect PPARG expression in formalin-fixed, paraffin-embedded (FFPE) UC human tissue specimens.
- Our data show that PPARG protein expression correlated with PPARG RNA expression in a retrospective cohort of archival tissue biospecimens from high-grade localized UC.

METHODS

FIGURE 1. PPARG immunohistochemical staining assay development paradigm

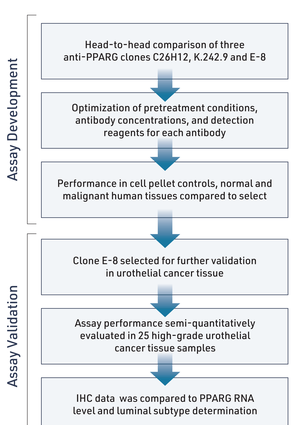

Immunohistochemistry

- Testing for PPARG was performed in formalin-fixed, paraffin-embedded (FFPE) human tissues using PPARg clone E-8 (Santa Cruz Biotechnology Cat. No. sc-7273), PPARG clone K.242.9 (ThermoFisher Cat. No. MA5-14889) and PPARG clone C26H12 (Cell Signaling Technology Cat. No. 2435s) for detection. Urothelial cancer tissues and control tissues, such as tonsil and testis, were used for assay validation. In addition, specificity of the PPARG staining was demonstrated in cell lysates, where PPARG expression level was confirmed by Western blot (HEK293, RT-112, BC-3C, 5637, HT1197, and UMUC9, Figure 1). For all three antibody clones, different concentrations were tested.

E-8 PPARG Clone

- Post validation, IHC using the E-8 PPARG clone was deployed and evaluated in a retrospective cohort of 25 high-grade localized, stage III-IV MIUC.
- *Methodology:* Epitope retrieval was performed on the Bond III using ER2 solution (Leica Biosystems, Cat. No. AR9640) heated to 100°C with enzymatic digestion with Proteinase K (BioGenex, Cat. No. HK8785K-GP) at 37°C. Primary incubation time was 1 hour at a concentration of 8.0 µg/mL. The location of the primary antibody was visualized using Leica detection reagents (Leica Biosystems, Cat. No. DS9800). After dehydration, slides were permanently coverslipped using cytoseal (ThermoFisher Scientific, Cat. No. 23244256 (8310-4)) and examined under a microscope to assess staining.
- *IHC Evaluation and Scoring:* Pathologist determined the percentage of tumor cells positive for PPARG staining (0% to 100%) and the average intensity of staining (0 to 3+) of the tumor cells. An H-score (range, 0 to 300) was assigned to each sample by multiplying the percentage of tumor cells positive for PPARG staining by the average intensity of staining.

RNAseq

- Gene expression values were normalized by transcripts-per-million (TPM). Molecular classification was performed using non-negative matrix factorization (NMF) rank 5 following the Robertson method3 derived from RNAseq in matched MIUC cases [n = 24].

Scan to View this Poster, Abstract #856

RESULTS

FIGURE 2. Staining cell lines with varied levels of PPARG to evaluate candidate antibody clones

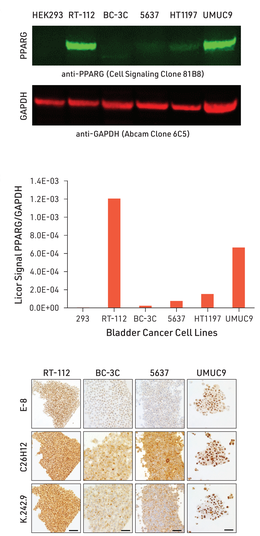

Staining cell lines with varied levels of PPARG supports the specificity of E-8 staining. **A.** Western blot showing the levels of PPARG in several cell lines. **B.** Quantitation of PPARG levels relative to GAPDH as a normalized control. Two UC cell lines with high levels of expression of PPARG (RT-112 and UMUC-9), and two UC cell lines with low levels of PPARG expression (BC-3C and 5637) were formalin fixed and paraffin embedded and stained with candidate antibodies. **C.** While the staining performance of the three antibodies in cell lines with high PPARG was similar and showed predominantly nuclear staining, the performance was different in cell lines with low levels of PPARG, where cytoplasmic staining was present in C26H12 and K.242.9 and was felt to be non-specific. The consistency between C26H12 and K.242.9 was not seen as corroborating specificity because they target the same epitope.

FIGURE 3. PPARG staining with candidate antibody clones in normal and cancer tissue

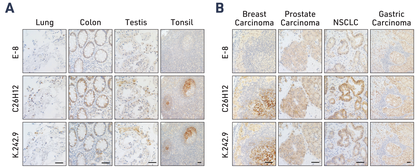

PPARG staining in normal and cancer tissue supports the specificity of the E-8 clone. Similar to the observations in cell lines, in tissues with high PPARG expression, as seen in gastric cancer samples, PPARG nuclear staining was seen across all antibodies. Differences in staining was more striking where there is low expression of PPARG. For example, in the epithelial cells of the colonic crypts, the Leydig cells of the testis, prostate cancer, and NSCLC cells, E-8 showed faint nuclear staining, while C26H12 and K.242.9 also showed strong cytoplasmic blush. Another difference observed between the antibodies was the membranous and cytoplasmic staining in germinal center of the tonsil and in the breast cancer sample. This staining pattern was interpreted as non-specific due to the cellular localization of the signal.

- PPARG expression with the E-8 clone showed a predominantly nuclear staining pattern, where 88% of urothelial cancer cases exhibited ≥1+ staining in ≥50% tumor cells (Figure 4).
- The E-8 clone detected a broad range of PPARG expression (Table 1).

TABLE 1. Distribution of nuclear PPARG expression based upon percent tumor area with ≥2+ staining and H-Score

Percent Score ≥2+ Staining [0-100%]	n, cases (%)	H-Score [0-300]	n, cases (%)
≥1	23 (92)	≥1	24 (96)
≥10	21 (84)	≥50	22 (88)
≥50	12 (48)	≥150	11 (44)
≥75	5 (20)	≥200	4 (16)
≥90	3 (12)	≥250	2 (8)

FIGURE 4. PPARG staining with clone E-8 in UC samples

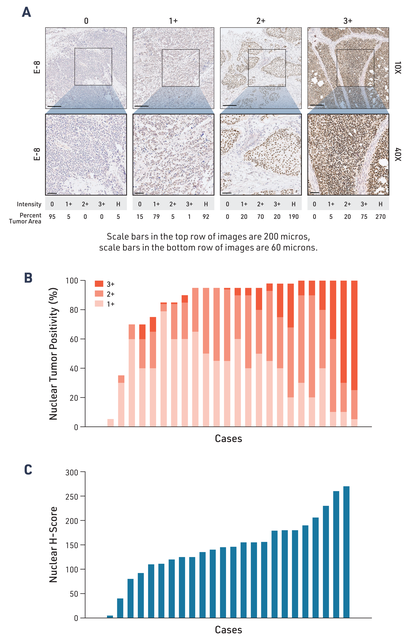

Clone E-8 demonstrated good sensitivity, range, and linearity. **A.** Example images at two magnifications of samples with a range of staining intensities. Below each pair of images are the semiquantitative staining scores assigned to each of the four slides shown, including the % tumor area with staining scored as 0, 1+, 2+, and 3+, and H-score (column labeled H). **B.** Distribution of % tumor area staining in our 25 sample urothelial cancer is graphed as stacked columns of the % tumor area with 1+ staining, 2+ staining, and 3+ staining. **C.** Calculated H-scores varied from 0 to 270 (Median H-Score = 146), where 64% of the cases (16 out of 25) showed a moderate PPARG expression with H-scores ranging between 100 and 200.

FIGURE 5. PPARG assayed by IHC shows strong correlation with mRNA expression of PPARG in UC samples

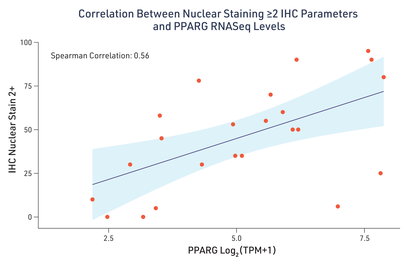

PPARG expression determined by IHC staining with antibody clone E-8 quantitated based upon the % tumor area with 2+ or greater staining correlated with RNA expression levels from RNAseq data [$\log_2$TPM+1] [Spearman r = 0.56] [p-value <0.01]. 24 of the 25 samples had associated RNA sequencing data with acceptable quality and were included in this analysis.

FIGURE 6. Luminal UC samples have significantly higher PPARG mRNA expression levels

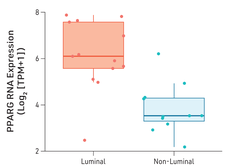

Similarly to previous data[2,5], 54.2% of the cases in this cohort were of luminal lineage (13 out of 24). The median RNA expression level of PPARG was significantly higher in the luminal subgroup compared to the non-luminal subgroup (6.1 $\log_2$[TPM+1] vs 3.53 $\log_2$[TPM+1], p <0.01).

CONCLUSION

These data show the IHC assay is sensitive and specific for the detection of PPARG expression in advanced UC with utility to identify patients with potential to respond to FX-909, a first-in-class PPARG-targeting agent[4].

References: **1.** Sims R, New Drugs on the Horizon: Part 2, 16th April 2023, AACR, Orlando, Fl; **2.** Motley W, et al. *Eur J Cancer* 2022 174(S1): S119; **3.** Robertson AG, et al. *Cell* 2017 171(3): 540-556.e25; **4.** Iyer G, et al. Trials in Progress, 26th January 2024, ASCO GU Cancers Symposium, San Francisco, CA; **5.** Kirov S, Molecular Targets and Cancer Therapeutics, 13th October 2023, AACR-NCI-EORTC, Boston, MA.